BNL-229973-2026-TECH

Comments on the paper "Eliminating beam-induced depolarizing effects in the hydrogen jet target for high-precision proton beam polarimetry at the Electron-Ion Collider" (Part II)

A. Poblaguev

June 2026

Electron-Ion Collider

Brookhaven National Laboratory

U.S. Department of Energy

USDOE Office of Science (SC), Nuclear Physics (NP)

Comments on the paper “Eliminating beam-induced depolarizing effects in the hydrogen jet target for high-precision proton beam polarimetry at the Electron-Ion Collider [1]” (Part II)

A. A. Poblaguev*
Brookhaven National Laboratory, Upton, New York 11973, USA
(Dated: July 15, 2026)

In this note, additional critical comments on the recent publication by F. Rathmann *et al.*, Phys. Rev. Accel. Beams 29, 021001 (2026), are presented.

Recently, Ref. [1] claimed that the beam-induced depolarization of the Polarized Atomic Hydrogen Gas Jet Target (HJET) at the future Electron-Ion Collider (EIC) would inevitably be large for a 120 mT holding field, corresponding to the value currently used at the Relativistic Heavy Ion Collider (RHIC).

This conclusion was challenged in Ref. [2], which presented an alternative evaluation of the beam-induced depolarization for the EIC HJET and demonstrated that the depolarization had been significantly overestimated in Ref. [1]. The methodology employed in Ref. [1] was further examined in the critical review of Ref. [3]. However, that review focused primarily on the overestimation of the depolarization, leaving several other incorrect statements in Ref. [1] unaddressed.

In this note, we discuss some of these additional inaccuracies.

A. Molecular contamination in atomic beams

In Appendix A of Ref. [1], it is stated that

> The approach used in Ref. [5] to determine the molecular fraction by simply turning off the dissociator is ill-fated, as it does not produce defocused atoms and, as such, does not lend itself as a method to realistically estimate the molecular content in the target.

This statement is inaccurate and misleading.

In Ref. [5], a background-subtraction method was developed that accurately accounts for the contribution of molecular hydrogen originating from defocused atoms that recombine on the inner surfaces of the sextupole magnets. As explicitly discussed in that work, this method is, by construction, insensitive to the small molecular fraction originating directly from the nozzle. To evaluate this latter contribution, a dedicated measurement with the dissociator turned off was performed. Thus, the two procedures employed in Ref. [5] address different physical sources of molecular hydrogen and are complementary rather than mutually exclusive.

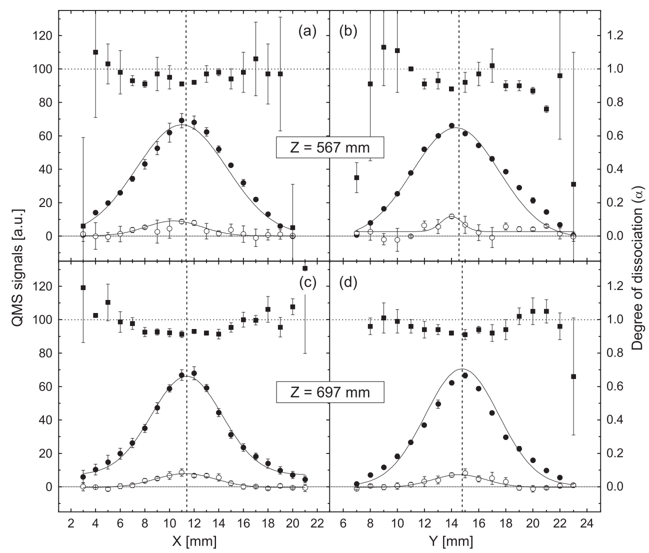

FIG. 1. (Fig. 24 in Ref. [4]) Spatial distributions of H_1 (●), H_2 (○), and the degree of dissociation (■), averaged over 3 mm-wide bands in the xz and yz planes, respectively (here the z-axis is the geometrical axis of the ABS).

Furthermore, in Appendix A (of Ref. [1]), the molecular hydrogen content of the target is estimated using a graphical analysis (shown in Fig. 1) of quadrupole mass spectrometer (QMS) measurements performed at the ANKE experiment [4]. By considering measurements at multiple transverse positions in the x and y directions (perpendicular to the atomic beam) at a distance of 697 mm downstream of the last sextupole magnet, the resulting degree of dissociation of the atomic beam is estimated (Eq. (A1) of Ref. [1]) as

$$\alpha_{[1]} = \frac{1}{1-2\,\rho_m/\rho_a} = 0.934 \pm 0.006, \tag{1}$$

where ρ_a and ρ_m are the measured integrated densities of atomic and molecular hydrogen, respectively, within a 10 mm aperture of the beam.

It should be emphasized that the quoted uncertainty in Eq. (1) is in significant disagreement with the accuracy

---

* poblaguev@bnl.gov

reported in Ref. [4], from which the data were taken:

$$\bar{\alpha}_{[4]} = 0.95 \pm 0.04. \tag{2}$$

A cursory inspection of the graphs used for the estimate in Appendix A suggests that this discrepancy most likely arises from the neglect of systematic uncertainties in the analysis presented there. The following simplified consideration illustrates possible sources of systematic error in the analysis of Ref. [1].

Assuming that the transverse density of the atomic beam is

$$\rho_a(x,y) = \frac{n_a}{2\pi\sigma_a^2}\exp\left(-\frac{x^2+y^2}{2\sigma_a^2}\right), \tag{3}$$

and a similar expression holds for the molecular hydrogen density parameterized by n_m and σ_m, the degree of dissociation for a sufficiently large aperture is given by

$$\alpha = \frac{1}{1+2n_m/n_a}. \tag{4}$$

Within this approximation, the dissociation profile along the x-axis depends on the following ratio:

$$\frac{\rho_m(x,0)}{\rho_a(x,0)} = \frac{n_m}{n_a}\times\frac{\sigma_a^2}{\sigma_m^2}\exp\left[-\frac{x^2}{2\sigma_m^2}\left(1-\frac{\sigma_m^2}{\sigma_a^2}\right)\right]. \tag{5}$$

The experimental distributions of $\rho_m(x)/\rho_a(x)$ and $\rho_m(y)/\rho_a(y)$ shown in Fig. 1 therefore indicate that $\sigma_m < \sigma_a$. A similar conclusion also follows from a visual comparison of the ρ_a and ρ_m density distributions in Fig. 1.

However, if the dominant source of molecular hydrogen is recombination of defocused atoms on the inner surfaces of the sextupole magnets [1], one would instead expect $\sigma_m \gg \sigma_a$ [5]. For molecular hydrogen originating directly from the nozzle, one expects $\sigma_m \gtrsim \sigma_a$ [5].

We are thus led to conclude that the molecular hydrogen density profiles $\rho_m(x,y)$ extracted in Ref. [4] are either not representative of those at RHIC HJET or are significantly affected by systematic uncertainties (e.g. background contributions) in the measurement.

Given the relatively large uncertainty of 4% in the degree of dissociation reported in Eq. (2), the presence of a negligible (or even vanishing) molecular hydrogen component cannot be excluded. This, in turn, implies substantial systematic uncertainties in the experimental determination of $\rho_m(x,y)$.

Notably, this result itself calls into question the capability of QMS-based methods to determine the molecular hydrogen fraction in the atomic beam with sub-percent accuracy, as required for the EIC.

B. Doppler broadening of the transition frequency

It is stated in Sec. V.B.1 of Ref. [1] that the velocity distribution of the atomic beam introduces significant broadening mechanisms that affect the resonance conditions.

Typically, Doppler broadening of an electromagnetic wave arises from the velocity distribution of the emitters. In the present case, however, the beam-induced magnetic field propagates along the z-axis (following the beam bunches), while the hydrogen atoms move with a nearly fixed velocity $v_a \sim 1800\,\mathrm{m/s}$ along the y-axis. This configuration corresponds to a transverse Doppler effect, which modifies the oscillating magnetic-field frequency f in the atomic rest frame as

$$f \to f \times \left(1 - \frac{v_a^2}{c^2}\right). \tag{6}$$

For the $|1\rangle \to |2\rangle$ transition harmonic, this corresponds to an effective shift of the holding field of approximately 20 pT, with even smaller effects for other harmonics. Such corrections are entirely negligible.

C. The stimulated transition rate

In Sec. VI.D of Ref. [1], it was claimed that the quantum-mechanical framework presented in Appendix C of Ref. [1] was used to quantify the depolarization effects. As follows directly from Appendix C, the stimulated transition rate for a specific hyperfine transition $|i\rangle \to |j\rangle$ is given by

$$\Gamma_{ij}(f) = \frac{2\pi}{\hbar}\left|\langle i|H_1|j\rangle\right|^2 S(f)V_{\mathrm{int}}, \tag{7}$$

where $S(f)$ is the spectral power density, and the matrix element $\langle i|H_1|j\rangle$ is assumed to be time independent.

However, in the practical calculations presented in Sec. VI.D, the well-known Rabi formula for the resonant transition probability,

$$\Gamma_{ij} = \sin^2\left(\frac{\omega_R(f)\tau_{\mathrm{int}}}{2}\right), \tag{8}$$

was used instead. Here, $\omega_R(f)$ is the Rabi frequency, and τ_{int} is the interaction time, i.e., the time during which the atom remains under resonant conditions.

Thus, the declared calculation method appears to be irrelevant to the method actually used.

In the second example discussed in Sec. VI.D, the interaction time $\tau_{\mathrm{int}} \approx 0.94\,\mu\mathrm{s}$ was determined from the time required for an atom to traverse the region where the induced field exceeds $\Delta B_h^{\mathrm{pk}} = 2.0\,\mathrm{mT}$. However, it was overlooked that, due to the bunch structure of the beam, with temporal rms width $\sigma_t = 0.2\,\mathrm{ns}$ and bunch period $\tau_b = 11.027\,\mathrm{ns}$, the condition $\Delta B_h(t) > 2.0\,\mathrm{mT}$ is satisfied only during a small fraction of the bunch period,

$$\frac{2\sigma_t}{\tau_b}\sqrt{2\ln\left(\frac{B_m}{\Delta B_h^{\mathrm{pk}}}\right)} \approx 0.033, \tag{9}$$

where $B_m = 3.03\,\mathrm{mT}$ is the maximum peak value of the beam-induced magnetic field. Therefore, the value of τ_{int} should be reduced by at least a factor of 30.

Moreover, for a more accurate evaluation of τ_{int}, only the time intervals during which the frequency of the resonant harmonic of the induced field is consistent with the transition frequency should be included. The latter depends on the holding field value, including the spatially varying beam-induced component parallel to the static field, within the corresponding Rabi-frequency width. Such a treatment would lead to an additional reduction of the effective interaction time τ_{int}.

D. Calculation of the effective power broadening

In Sec. V.B.1, the effective power broadening was introduced as a standard deviation derived from the previously calculated Rabi frequency f_R:

$$\sigma_f^{\mathrm{power}} = \frac{f_R}{2\sqrt{2\ln 2}}. \tag{10}$$

The factor $2\sqrt{2\ln 2} \approx 2.36$ is readily recognized as the ratio between the full width at half maximum (FWHM) and the rms width of a Gaussian distribution.

However, for small detuning Δf, the transition probability in the Rabi process is given by

$$\frac{f_R^2}{f_R^2 + \Delta f^2} \sin^2\left(\pi t \sqrt{f_R^2 + \Delta f^2}\right). \tag{11}$$

As a function of Δf, the corresponding resonance curve has an FWHM equal to $2f_R$, rather than f_R. Therefore, the value of $\sigma_f^{\mathrm{power}}$ in Eq. (10) should be multiplied by a factor of 2.

E. Hyperfine-state eigenenergies for the complete Hamiltonian

The dependence of the ground-state hydrogen hyperfine energy levels on the holding field B_h, expressed as functions $E_{|i\rangle}(x)$ of the dimensionless parameter

$$x = \frac{-2\mu_e B_h}{E_{\mathrm{hfs}}} = \frac{g_J \mu_B B_h}{E_{\mathrm{hfs}}}, \tag{12}$$

is presented in Eq. (11) of Ref. [1]. However, these expressions were derived neglecting the nuclear magnetic moment $\mu_p = g_I \mu_N / 2$.

A more accurate treatment was attempted in Appendix B of Ref. [1], where the complete Hamiltonian, expressed in terms of the parameters x and $y = 2g_I \mu_N B_h / E_{\mathrm{hfs}}$, is given in Eq. (B5). However, a comparison of Eqs. (B1), (B2), and (B3) indicates that the sign of the term $g_I \mu_N I_z B_h$ in Eq. (B3) was written incorrectly. Therefore, in Eq. (B5), one should replace

$$y \to -2y, \tag{13}$$

where the factor of 2 arises from redefining the parameter y in a form analogous to that used for x:

$$y = \frac{g_I \mu_N B_h}{E_{\mathrm{hfs}}}. \tag{14}$$

Noting that, for $y = 0$, Eq. (B5) reproduces the energy levels given in Eq. (11) of Ref. [1], one immediately obtains

$$E_{|1\rangle}(x) = \frac{E_{\mathrm{hfs}}}{2}\left[-\frac{1}{2} + 1 + (x - y)\right], \tag{15}$$

$$E_{|2\rangle}(x) = \frac{E_{\mathrm{hfs}}}{2}\left[-\frac{1}{2} + \sqrt{1 + (x + y)^2}\right], \tag{16}$$

$$E_{|3\rangle}(x) = \frac{E_{\mathrm{hfs}}}{2}\left[-\frac{1}{2} + 1 - (x - y)\right], \tag{17}$$

$$E_{|4\rangle}(x) = \frac{E_{\mathrm{hfs}}}{2}\left[-\frac{1}{2} - \sqrt{1 + (x + y)^2}\right], \tag{18}$$

in exact agreement with Eq. (12.37) of Ref. [6].

Since $y/x \approx 0.0015$, the energies $E_{|2\rangle}$ and $E_{|4\rangle}$ can be approximated, with relative accuracy $\mathcal{O}(2 \times 10^{-6})$, as

$$E_{|2\rangle}(x) \approx \frac{E_{\mathrm{hfs}}}{2}\left[-\frac{1}{2} + \sqrt{1 + x^2} + y\frac{x}{\sqrt{1 + x^2}}\right], \tag{19}$$

$$E_{|4\rangle}(x) \approx \frac{E_{\mathrm{hfs}}}{2}\left[-\frac{1}{2} - \sqrt{1 + x^2} - y\frac{x}{\sqrt{1 + x^2}}\right]. \tag{20}$$

Thus, in addition to the incorrect sign of y, the dependence of the hyperfine energy levels $|2\rangle$ and $|4\rangle$ on y was also calculated incorrectly in the paragraph of Appendix B following Eq. (B5).

[1] F. Rathmann *et al.*, Phys. Rev. Accel. Beams **29**, 021001 (2026), arXiv:2508.01366 [physics.acc-ph].

[2] A. A. Poblaguev, Nucl. Instrum. Meth. A **1091**, 171776 (2026), arXiv:2601.17220 [physics.ins-det].

[3] A. Poblaguev, *Comments on the paper "Eliminating beam-induced depolarizing effects in the hydrogen jet target for high-precision proton beam polarimetry at the Electron-Ion Collider"*, Tech. Rep. BNL-229894-

2026-TECH (Brookhaven National Laboratory, 2026) arXiv:2606.30672 [physics.acc-ph].
[4] M. Mikirtychyants *et al.*, Nucl. Instrum. Meth. A **721**, 83 (2013), arXiv:1212.1840 [physics.ins-det].
[5] A. A. Poblaguev, A. Zelenski, G. Atoian, Y. Makdisi, and J. Ritter, Nucl. Instrum. Meth. A **976**, 164261 (2020), arXiv:2006.08393 [physics.ins-det].
[6] R. P. Feynman, R. B. Leighton, and M. Sands, *The Feynman Lectures on Physics, Vol. 3*, new millennium ed. (Basic Books, 2011).